



Titanium dioxide surface modified with both palladium and fluoride as an efficient photocatalyst for the degradation of urea



Hyoung-il Kim^a, Kitae Kim^b, Soona Park^c, Wooyul Kim^d, Seungdo Kim^c, Jungwon Kim^{c,*}

^a School of Civil and Environmental Engineering, Yonsei University, Seoul 03722, Republic of Korea

^b Korea Polar Research Institute (KOPRI), Incheon 21990, Republic of Korea

^c Department of Environmental Sciences and Biotechnology, Hallym University, Chuncheon, Gangwon-do 24252, Republic of Korea

^d Department of Chemical and Biological Engineering, Sookmyung Women's University, Seoul 04310, Republic of Korea

ARTICLE INFO

Keywords:

Photocatalysis
Titanium dioxide
Palladium loading
Fluoride complexation
Urea degradation

ABSTRACT

TiO₂ surface modified with both Pd nanoparticles and fluorides (F-TiO₂/Pd) was prepared and applied as a photocatalyst in the degradation of urea. Various surface analysis techniques, including X-ray photoelectron spectroscopy, high-resolution transmission electron microscopy, and energy-dispersive X-ray spectroscopy, were used to verify the coexistence of Pd nanoparticles and fluorides on the surface of TiO₂ in F-TiO₂/Pd. F-TiO₂/Pd showed a higher photocatalytic activity than those of bare TiO₂ and single-component-modified TiO₂ photocatalysts such as fluorinated TiO₂ (F-TiO₂) and Pd-loaded TiO₂ (Pd/TiO₂). The higher urea degradation efficiency of F-TiO₂/Pd is ascribed to the enhanced production of hydroxyl radicals ([•]OH) by the synergistic action of the surface Pd and fluoride. Pd nanoparticles and fluorides facilitate the transfer of valence band holes (h_{vb}⁺) and their reaction with water molecules, respectively, synergistically enhancing the production of [•]OH. The photocatalytic activity of F-TiO₂/Pd for the degradation of urea increased upon increasing the fraction of the fluorinated TiO₂ surface, which is higher at higher fluoride concentrations and lower pH. Although Pt/TiO₂ showed higher photocatalytic activity for the degradation of urea than those of Pd/TiO₂ and Au/TiO₂, the strong positive effect of fluoride complexation was only exhibited by Pd/TiO₂ (a slight positive effect and a negative effect were observed for Au/TiO₂ and Pt/TiO₂, respectively). As a result, the degradation of urea proceeded more rapidly in a UV-irradiated suspension of F-TiO₂/Pd than when any of other photocatalysts (i.e., bare TiO₂, Pd/TiO₂, F-TiO₂, Au/TiO₂, F-TiO₂/Au, Pt/TiO₂, and F-TiO₂/Pt) were used under the same conditions. The first-order degradation rate constants (*k*) of urea depending on the type of TiO₂ were as follows: 0.097 h⁻¹ for bare TiO₂, 0.158 h⁻¹ for Pd/TiO₂, 0.151 h⁻¹ for F-TiO₂, 0.351 h⁻¹ for F-TiO₂/Pd, 0.173 h⁻¹ for Au/TiO₂, 0.223 h⁻¹ for F-TiO₂/Au, 0.240 h⁻¹ for Pt/TiO₂, and 0.165 h⁻¹ for F-TiO₂/Pt, respectively. In addition, F-TiO₂/Pd proved to be stable in repeated urea degradation cycles.

1. Introduction

Heterogeneous photocatalysis has been extensively studied as an eco-friendly technology for water purification [1]. Among the various semiconductor photocatalysts, titanium dioxide (TiO₂) is regarded as one of the most viable photocatalysts because of its strong oxidation ability, low material cost, nontoxicity, and high chemical and photochemical stabilities [2–4]. UV irradiation of TiO₂ in the presence of water and oxygen generates various oxidizing species, such as valence band holes (h_{vb}⁺), hydroxyl radicals ([•]OH), superoxide/hydroperoxyl radicals (O₂^{•-}/HO₂[•]), and hydrogen peroxide (H₂O₂), through the photoexcitation of electrons from the valence band (VB) to the conduction band (CB), i.e., the generation of electron-hole pairs [5,6].

Among these oxidizing species, h_{vb}⁺ and [•]OH, which have higher oxidation powers than O₂^{•-}/HO₂[•] and H₂O₂, are primarily involved in the degradation of aquatic pollutants [7].

A variety of surface modifications have been applied to TiO₂ with the aim of increasing the production of oxidizing species, thus improving its practical viability for water treatment [8–12]. Metal loading [13–15], especially with platinum (Pt), and anion complexation [16–19], especially with fluoride (F⁻), are commonly used TiO₂-surface-modification methods. Metal nanoparticles on the surface of TiO₂ enhance the production of oxidizing species by retarding the recombination of photogenerated electron-hole pairs and promoting electron transfer from the TiO₂ CB to oxygen [20]. Furthermore, the production of [•]OH is increased by the complexation of anions on the

* Corresponding author.

E-mail address: jwk@hallym.ac.kr (J. Kim).

<https://doi.org/10.1016/j.seppur.2018.07.058>

Received 23 April 2018; Received in revised form 9 July 2018; Accepted 22 July 2018

Available online 24 July 2018

1383-5866/ © 2018 Elsevier B.V. All rights reserved.

TiO₂ surface because the substitution of hydroxyl groups on the TiO₂ surface by anions ($\text{Ti-OH} + \text{A}^- \rightarrow \text{Ti-A} + \text{OH}^-$) reduces the generation of surface-bound $\cdot\text{OH}$ ($\text{Ti-OH} + h\nu_{\text{vb}}^+ \rightarrow \text{Ti}^-\cdot\text{OH}$), which is likely to react with the TiO₂ CB electrons, and facilitates the generation of mobile $\cdot\text{OH}$ ($\text{Ti-A} + h\nu_{\text{vb}}^+ + \text{H}_2\text{O} \rightarrow \text{Ti-A} + \text{mobile } \cdot\text{OH} + \text{H}^+$), which can diffuse from the TiO₂ surface without reacting with CB electrons [21]. It has also been reported that the TiO₂ surface modified with both Pt nanoparticles and fluorides (F-TiO₂/Pt) shows unique behaviors, such as anoxic photocatalytic degradation of aqueous phenolic pollutants coupled with the production of hydrogen [22,23] and a high resistance to deactivation during the photocatalytic degradation of gaseous toluene [24]. On F-TiO₂/Pt, surface fluorides inhibit the adsorption of phenolic intermediates (oxidized phenolic pollutants) and the generation of surface-bound $\cdot\text{OH}$ (Both phenolic intermediates adsorbed on the surface and surface-bound $\cdot\text{OH}$ immediately react with CB electrons in anoxic conditions). Under this situation, the trapped electrons in Pt can preferentially react with protons or water molecules and mobile $\cdot\text{OH}$ can oxidize phenolic pollutants away from the surface of F-TiO₂/Pt [22,23].

Although urea itself is not toxic, it has harmful indirect effects on aquatic organisms and humans. Urea causes algal bloom in coastal waters as a source of nitrogen nutrients [25] and induces the formation of toxic nitrogen-containing compounds in chlorine-mediated disinfection processes [26]. Large amounts of urea-containing industrial wastewater are produced by industrial activities such as fertilizer, plastics, feeds, and explosives manufacturing that use urea as a chemical reagent [27]. In addition, human urine, which contains urea in the range 9.3–23.3 g/L, acts as a source of urea in domestic wastewater [28]. Recently, urea has received much research attention as an aquatic pollutant. The recycling of human urine into clean water on the International Space Station (ISS) virtually eliminates the need to supply water from the Earth, enabling longer stays and an increased number of crew members [29]. The degradation of urea in human urine is a vital step in water recycling process on the ISS. Thus, various techniques for the degradation of urea have recently been developed, including biological [30], electrochemical [31,32], bioelectrochemical [33,34], photoelectrochemical [35], and photocatalytic methods [36,37].

Urea is readily biodegradable. However, the operation of biological processes in the ISS is very difficult, which requires the development of simple and easy-to-handle methods for the degradation of urea. Although the photocatalytic degradation of urea using bare TiO₂ and Pt-loaded TiO₂ (Pt/TiO₂) photocatalysts has been previously reported [36,37], developing more efficient photocatalysts for the degradation of urea remains a challenging issue. In this study, the TiO₂ surface modified with both palladium and fluoride (F-TiO₂/Pd) was prepared and applied as a photocatalyst for the degradation of urea. The application of F-TiO₂/Pd for the degradation of pollutants in the presence of oxygen has not been reported. Characterization of F-TiO₂/Pd was performed by various surface analysis methods. The photocatalytic degradation of urea over F-TiO₂/Pd under UV irradiation was assessed and compared with that over bare TiO₂, Pd-loaded TiO₂ (Pd/TiO₂), and fluorinated TiO₂ (F-TiO₂). Urea degradation kinetics in UV-irradiated suspensions of F-TiO₂/Pd were measured under various experimental conditions. Furthermore, the effects of fluoride complexation of different metal-loaded TiO₂ photocatalysts on their urea degradation activities were investigated. Finally, the synergistic effect of fluoride complexation and Pd loading on the TiO₂ surface was discussed in terms of the production of $\cdot\text{OH}$ and the degradation of urea.

2. Experimental

2.1. Chemicals

Chemicals used in this study include urea (NH₂CONH₂, Sigma-Aldrich, $\geq 99.0\%$), sodium fluoride (NaF, Sigma-Aldrich, $\geq 99.0\%$), sodium nitrate (NaNO₃, Sigma-Aldrich, $\geq 99.0\%$), ammonium chloride

(NH₄Cl, Sigma-Aldrich, $\geq 99.0\%$), urease from *Canavalia ensiformis* (Jack bean) (type III, Sigma, 15,000–50,000 units/g solid), coumarin (C₉H₆O₂, Sigma, $\geq 99.0\%$), chloroplatinic acid hydrate (H₂PtCl₆·xH₂O, Aldrich, $\geq 99.9\%$), palladium chloride (PdCl₂, Aldrich, $\geq 99.9\%$), gold chloride hydrate (HAuCl₄·xH₂O, Aldrich, $\geq 99.995\%$), methanol (CH₃OH, Wako, $\geq 99.8\%$), sodium carbonate (Na₂CO₃, Sigma-Aldrich, $\geq 99.0\%$), sodium bicarbonate (NaHCO₃, Sigma-Aldrich, $\geq 99.7\%$), and methanesulfonic acid (CH₃SO₃H, Sigma-Aldrich, $\geq 99.5\%$). Aeroxide P25 (Evonik) (molar ratio of anatase to rutile = 4.85:1; BET surface area = 60 m²/g) [38] was used as the TiO₂ material. All solutions were prepared in deionized water (18.3 MΩ·cm) made using a Human-Power I + water purification system (Human Corporation).

The artificial urine solution was synthesized using various chemicals such as urea (200.0 μM), potassium phosphate monobasic (KH₂PO₄, Sigma-Aldrich, $\geq 99.0\%$, 14.8 μM), sodium sulfate (Na₂SO₄, Sigma-Aldrich, $\geq 99.0\%$, 7.8 μM), sodium citrate tribasic dihydrate (Na₃C₆H₅O₇·2H₂O, Sigma-Aldrich, $\geq 99.0\%$, 1.1 μM), creatinine (C₄H₇N₃O, Sigma-Aldrich, $\geq 98\%$, 4.7 μM), sodium oxalate (Na₂C₂O₄, Sigma-Aldrich, $\geq 99.5\%$, 0.1 μM), potassium chloride (KCl, Sigma-Aldrich, $\geq 99.5\%$, 10.3 μM), ammonium chloride (NH₄Cl, Sigma-Aldrich, $\geq 99.5\%$, 9.0 μM), magnesium chloride hexahydrate (MgCl₂·6H₂O, Sigma-Aldrich, $\geq 99.0\%$, 1.5 μM), sodium chloride (NaCl, Sigma-Aldrich, $\geq 99\%$, 37.8 μM), and calcium chloride dihydrate (CaCl₂·2H₂O, Sigma-Aldrich, $\geq 99.0\%$, 2.1 μM) [39].

2.2. Preparation and characterization of photocatalysts

Metal loading on the surface of TiO₂ was performed by a photo-deposition method [40]. An aqueous suspension of TiO₂ (0.5 g/500 mL) was irradiated with a 200 W Hg lamp in the presence of the appropriate metal precursor (palladium chloride for Pd, chloroplatinic acid hydrate for Pt, and gold chloride hydrate for Au) and methanol as an electron donor (1 M). After the TiO₂ suspension was irradiated for 30 min, the metal-loaded TiO₂ powder was collected by filtration, washed with deionized water, and dried in an oven. The amount of metal loading on the TiO₂ surface was estimated by measuring the concentration of the metal precursor remaining in the filtrate solution using inductively coupled plasma-atomic emission spectroscopy (ICP-AES, Spectro). The mass ratio of metal to TiO₂ in the metal-loaded TiO₂ powders was approximately 1:100.

The complexation of fluoride on the TiO₂ (or metal-loaded TiO₂) surface was performed by a ligand exchange method [41]. NaF was added to a suspension of TiO₂ (or metal-loaded TiO₂). Then, the pH of the suspension was lowered using concentrated HClO₄ solution to induce ligand exchange between fluoride anions in the solution and hydroxyl groups on the TiO₂ surface. F-TiO₂ (or F-TiO₂/metal) prepared in solution was directly used without filtration and drying for the measurement of its photocatalytic activity.

F-TiO₂ (or F-TiO₂/Pd) sample for surface analysis was prepared as follows. NaF (3 mM) was added to an aqueous TiO₂ (or Pd/TiO₂) suspension (17.5 mg/35 mL), and the pH of the suspension was lowered to 4.0. After the suspension was stirred for 30 min, the F-TiO₂ (or F-TiO₂/Pd) powder was collected by filtration and dried at room temperature. The surface atomic compositions of bare TiO₂, Pd/TiO₂, F-TiO₂, and F-TiO₂/Pd were investigated using X-ray photoelectron spectroscopy (XPS, Thermo Scientific Theta Probe) with the Al Kα line (1486.6 eV) as the X-ray source. The elemental distribution on the F-TiO₂/Pd surface was explored by high-resolution transmission electron microscopy (HRTEM) and energy-dispersive X-ray (EDX) analyses using a JEOL JEM-2100F microscope at an accelerating voltage of 200 kV.

2.3. Photocatalytic experiments and chemical analyses

The photocatalyst powder (bare TiO₂ or metal-loaded TiO₂ (usually Pd/TiO₂)) was dispersed in deionized water, and an aliquot of a urea stock solution was added to the photocatalyst suspension to give the

desired urea concentration (photocatalyst mass = 17.5 mg, [urea] = 200 μ M, and solution volume = 35 mL). For surface fluoride complexation, NaF was added to the photocatalyst suspension (usually [NaF] = 3 mM). The pH of the photocatalyst suspension was adjusted using concentrated HClO₄ or NaOH solution (usually pH = 4.0). The photocatalyst suspension was stirred for 30 min in the dark to reach adsorption/desorption equilibrium and the uniform distribution of urea and fluorides within the system.

A 300 W Xe arc lamp (Oriel) was used as a light source. The light beam was focused onto a cylindrical Pyrex reactor (40 mL) through a 5 cm IR water filter and a cutoff filter ($\lambda > 320$ nm). The incident light intensity was measured using ferrioxalate actinometry [42] and estimated to be about 1.85×10^{-3} einstein $\text{min}^{-1} \text{L}^{-1}$. The reactor on a magnetic stirrer was open to ambient conditions to prevent the depletion of dissolved oxygen. Sample aliquots (1 mL) were withdrawn from the UV-irradiated reactor at predetermined time intervals using a syringe and filtered through a 0.45 μ m PTFE syringe filter (Millipore) to remove the photocatalyst particles. Multiple (two or more) experiments were performed for a given set of conditions to confirm the reproducibility of the data.

The concentration of urea was determined indirectly by measuring the concentration of ammonium (NH_4^+) generated from the hydrolysis of urea by urease ($\text{NH}_2\text{CONH}_2 + \text{H}_2\text{O} + 2\text{H}^+ + \text{urease} \rightarrow \text{CO}_2 + 2\text{NH}_4^+$) [43]. Samples containing urease (0.5 mL of sample and 0.1 mL of urease (0.12 g/100 mL)) were incubated in a water bath at 50 °C for 20 min, kept at room temperature for 30 min, and then analyzed. Samples without urease (0.5 mL of sample and 0.1 mL of deionized water) were used as a reference. The quantitative analysis of NH_4^+ and nitrate (NO_3^-) was performed using an ion chromatograph (IC, Dionex ICS-1100) equipped with a Dionex IonPac AS14 column (4 mm \times 250 mm), a Dionex IonPac CS12A column (4 mm \times 250 mm), and a conductivity detector. A binary mixture of sodium carbonate (3.5 mM) and sodium bicarbonate (1 mM) and a methanesulfonic acid solution (20 mM) were used as the eluents for the analysis of NO_3^- and NH_4^+ , respectively. The concentration of total organic carbon (TOC, total carbon – inorganic carbon) was measured using a TOC analyzer (Shimadzu TOC-L_{CPH}) equipped with a nondispersive IR sensor as a CO₂ detector.

The production of $\cdot\text{OH}$ in the UV-irradiated photocatalyst suspension was measured by a chemical trapping method using coumarin (1 mM) as a chemical probe [44]. The production of 7-hydroxycoumarin generated from the reaction of coumarin with $\cdot\text{OH}$ (coumarin + $\cdot\text{OH} \rightarrow$ 7-hydroxycoumarin) was monitored using a spectrofluorometer (Shimadzu RF-5301) by measuring the fluorescence emission intensity at 460 nm under excitation at 332 nm.

3. Results and discussion

3.1. Characterization of TiO₂ surface modified with both Pd and fluoride (F-TiO₂/Pd)

The surface atomic composition of F-TiO₂/Pd was examined using X-ray photoelectron spectroscopy (XPS). Those of Pd/TiO₂, F-TiO₂, and bare TiO₂ were also examined as references and are included in Fig. 1. The XPS spectra of the F-TiO₂/Pd sample show Pd peaks with binding energies of 335 eV (for Pd 3d_{5/2}) and 340 eV (for Pd 3d_{3/2}) and a F peak with a binding energy of 684 eV (for F 1s), which are consistent with metallic Pd loaded [45] and fluoride adsorbed on the surface of TiO₂ [46], respectively.

Fig. 2 shows HRTEM image, selected-area EDX spectrum, and elemental mapping images of a F-TiO₂/Pd sample. Pd elemental spots exist as clusters with sizes in the range 2–5 nm on the TiO₂ surface (Fig. 2a). The Pd peak in selected-area EDX spectrum confirms that the dark spots are Pd nanoparticles (Fig. 2b). The distribution of F elemental spots is well scattered and exactly overlaps with those of the Ti and O elemental spots (Fig. 2c–e). These surface analysis results confirm the coexistence

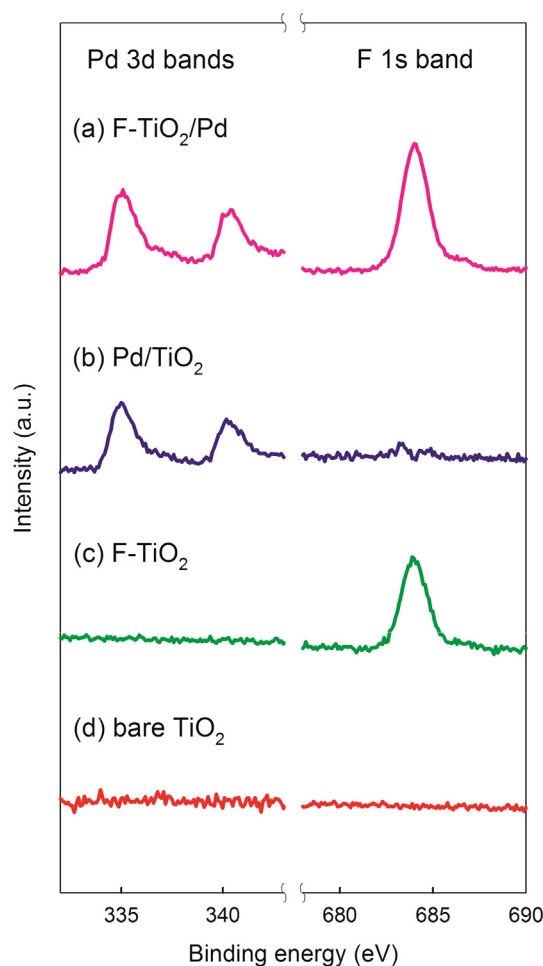


Fig. 1. Pd 3d and F 1s peaks in the XPS spectra of (a) F-TiO₂/Pd, (b) Pd/TiO₂, (c) F-TiO₂, and (d) bare TiO₂ powders.

of Pd nanoparticles and fluorides on the surface of TiO₂ in the F-TiO₂/Pd sample.

3.2. Synergistic effect of fluoride complexation and Pd loading on urea degradation

Fig. 3 shows the results for the photocatalytic degradation of urea and the concurrent production of its degradation products in suspensions of bare TiO₂, Pd/TiO₂, F-TiO₂, and F-TiO₂/Pd under UV irradiation. The degradation of urea followed first-order degradation kinetics with $R^2 > 0.98$ in all cases. Pd loading on the TiO₂ surface enhanced the photocatalytic activity for the degradation of urea. The degradation of urea was also accelerated by fluoride complexation on the TiO₂ surface. After 3 h of UV irradiation, 25%, 38%, and 36% of urea were degraded over bare TiO₂, Pd/TiO₂, and F-TiO₂, respectively (Fig. 3a–c). When TiO₂ was modified with both Pd and fluoride, the photocatalytic degradation of urea was most rapid. 67% of urea was degraded after 3 h of UV irradiation (Fig. 3d). These results clearly indicate that the two different surface modifications, i.e., Pd loading and fluoride complexation, have a synergistic effect on the TiO₂-based photocatalytic degradation of urea.

NH_4^+ and NO_3^- were generated in the course of urea degradation over both bare TiO₂ and surface-modified TiO₂. The nitrogen mass balance (i.e., $2 \times$ degraded [urea] = generated [NH_4^+] + generated [NO_3^-]) was satisfactory in all cases, which implies that the generation of other nitrogen species during urea degradation was negligible. The production of degradation products was in the order F-TiO₂/Pd > Pd/TiO₂ \approx F-TiO₂ > bare TiO₂. This trend is consistent with the data for

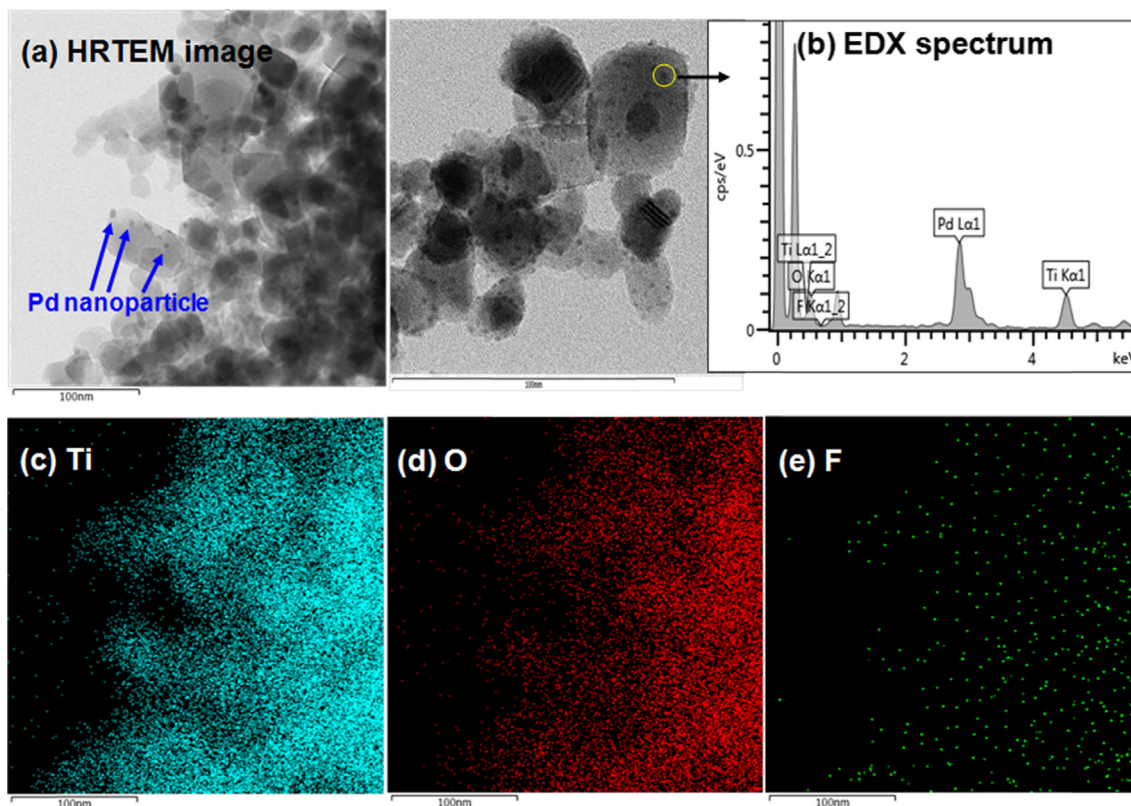


Fig. 2. (a) HRTEM image, (b) selected-area EDX spectrum, and (c) Ti, (d) O, and (e) F elemental mapping images of a F-TiO₂/Pd sample.

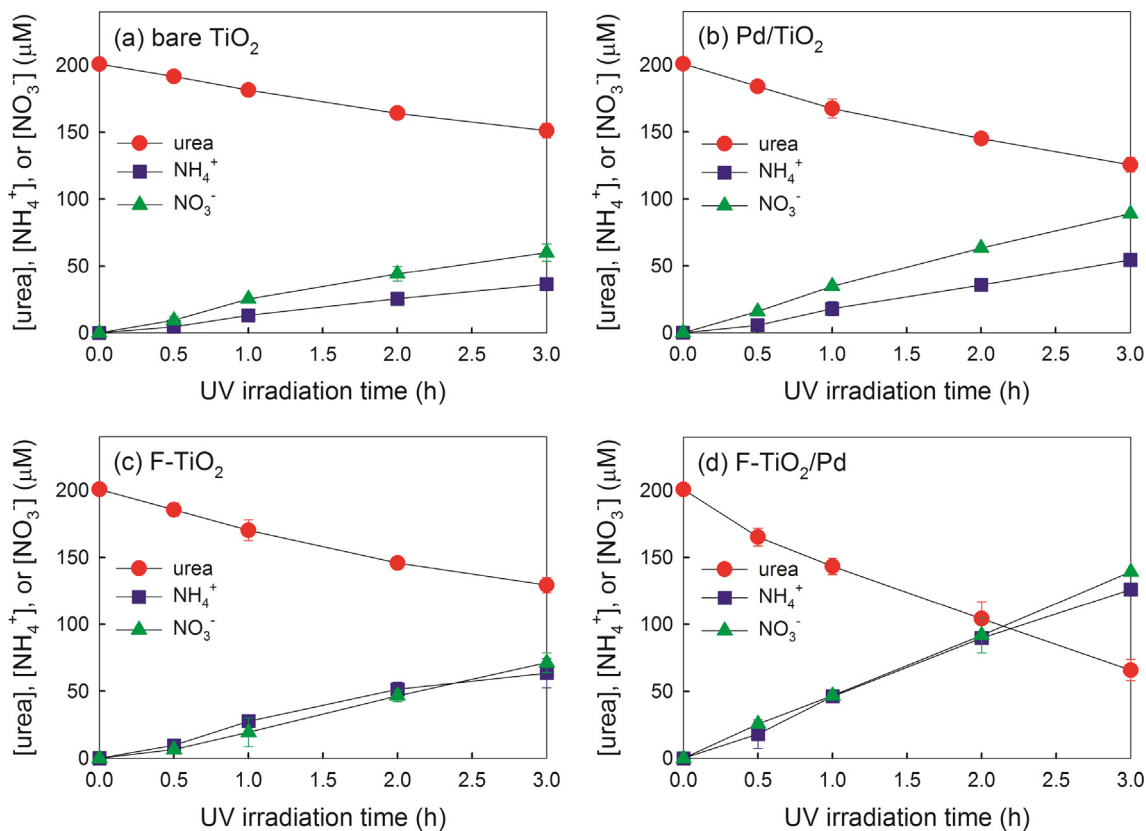


Fig. 3. Photocatalytic degradation of urea and the concurrent production of its degradation products in suspensions of (a) bare TiO₂, (b) Pd/TiO₂, (c) F-TiO₂, and (d) F-TiO₂/Pd under UV irradiation.

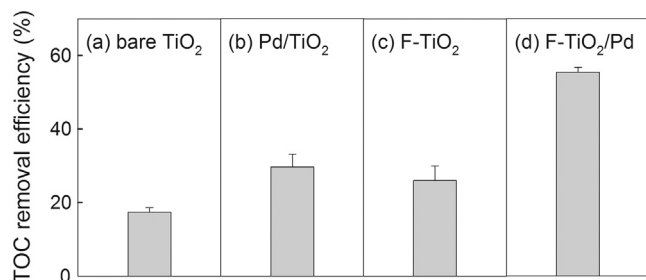


Fig. 4. TOC removal efficiency of urea in UV-irradiated suspensions of (a) bare TiO₂, (b) Pd/TiO₂, (c) F-TiO₂, and (d) F-TiO₂/Pd after 3 h.

the degradation of urea.

The degradation efficiency of the parent organic pollutant (i.e., the conversion efficiency of the parent organic pollutant to degradation products) is usually proportional to its mineralization efficiency (i.e., the conversion efficiency of the parent organic pollutant to CO₂). However, some cases deviate from this general trend. A photocatalyst exhibiting a high degradation efficiency may show a low mineralization efficiency toward a specific pollutant [47]. To confirm the superior photocatalytic activity of F-TiO₂/Pd for the removal of urea, the TOC removal (i.e., the mineralization) efficiency of urea over F-TiO₂/Pd after 3 h of UV irradiation was assessed and compared with those over bare TiO₂, F-TiO₂, and Pd/TiO₂ (Fig. 4). F-TiO₂/Pd showed a higher TOC removal efficiency than those of bare TiO₂, Pd/TiO₂, and F-TiO₂ (17% for bare TiO₂, 30% for Pd/TiO₂, 26% for F-TiO₂, and 55% for F-TiO₂/Pd). These results indicate that F-TiO₂/Pd is an efficient photocatalyst not only for the degradation but also for the mineralization of urea.

It has been reported that the photocatalytic degradation of urea on TiO₂ is primarily initiated by $\cdot\text{OH}$ attack, whereas h_{vb}^+ is hardly involved in the urea degradation process owing to the negligible adsorption of urea on the TiO₂ surface [36,37]. The adsorption of urea on Pd/TiO₂, F-TiO₂, and F-TiO₂/Pd as well as on bare TiO₂ was negligible. Therefore, the more rapid degradation of urea over surface-modified TiO₂ compared to that over bare TiO₂ should be ascribed to the enhanced production of $\cdot\text{OH}$ by Pd loading and/or fluoride complexation. Pd loading and fluoride complexation have no effect on the crystal structure of TiO₂ [19,45]. However, metal nanoparticles on TiO₂ surfaces retard photogenerated electron-hole recombination by serving as temporary electron reservoirs through the formation of Schottky barriers between the metal and the TiO₂ [20]. The retardation of electron-hole recombination facilitates h_{vb}^+ transfer to the surface hydroxyl groups of TiO₂ or water molecules, which enhances the production of $\cdot\text{OH}$. Fluoride anions on the TiO₂ surface also enhance the production of $\cdot\text{OH}$ by providing better conditions for the reaction of h_{vb}^+ with water molecules, i.e., the generation of mobile $\cdot\text{OH}$, which can largely avoid reaction with TiO₂ CB electrons by diffusing out from the TiO₂ surface [21]. The promotion of the reaction of h_{vb}^+ with water molecules by fluoride complexation is ascribed to two factors: (1) the reduced density of surface hydroxyl groups ($\text{Ti}-\text{OH}$) as a precursor of surface-bound $\cdot\text{OH}$, which enhances the reaction between h_{vb}^+ and water molecules (as a precursor of mobile $\cdot\text{OH}$) by inhibiting the reaction between h_{vb}^+ and $\text{Ti}-\text{OH}$ [47] and (2) the enhanced adsorption of water molecules owing to the photoinduced hydrophilicity of the fluorinated surface, which facilitates the reaction between h_{vb}^+ and water molecules [46]. The coexistence of Pd nanoparticles and fluorides on the surface of TiO₂ can synergistically enhance the production of $\cdot\text{OH}$ because Pd nanoparticles and fluorides facilitate h_{vb}^+ transfer from the TiO₂ bulk to the TiO₂ surface and from the TiO₂ surface to water molecules, respectively.

In order to provide direct evidence for the surface modification-enhanced $\cdot\text{OH}$ production and the synergistic effect of Pd loading and fluoride complexation on $\cdot\text{OH}$ production, the generation of $\cdot\text{OH}$ in

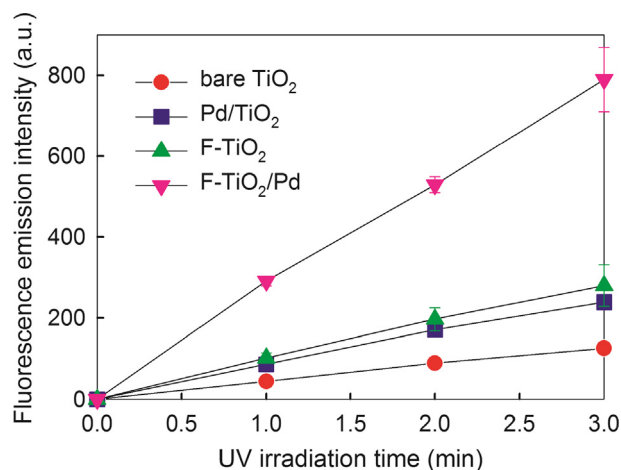


Fig. 5. Time profiles of the production of 7-hydroxycoumarin from coumarin in suspensions of bare TiO₂, Pd/TiO₂, F-TiO₂, and F-TiO₂/Pd under UV irradiation.

suspensions of bare TiO₂, Pd/TiO₂, F-TiO₂, and F-TiO₂/Pd under UV irradiation was monitored and compared (Fig. 5). The production of $\cdot\text{OH}$ is proportional to the production of 7-hydroxycoumarin in the presence of coumarin [44]. The production of $\cdot\text{OH}$ (i.e., the fluorescence emission intensity of 7-hydroxycoumarin) increased linearly with UV irradiation time not only over bare TiO₂ but also over surface-modified TiO₂. Pd/TiO₂ and F-TiO₂ produced more $\cdot\text{OH}$ than bare TiO₂. In addition, the production of $\cdot\text{OH}$ over F-TiO₂/Pd was much higher than those over Pd/TiO₂ and F-TiO₂, which implies that the surface Pd nanoparticles and fluorides exert a synergistic effect on the production of $\cdot\text{OH}$. Overall, the higher photocatalytic activity of F-TiO₂/Pd than those of bare TiO₂, Pd/TiO₂, and F-TiO₂ for the degradation of urea is ascribed to the enhanced production of $\cdot\text{OH}$ by the synergistic action of surface Pd and fluoride.

3.3. Urea degradation kinetics on F-TiO₂/Pd under various conditions

The complexation of fluoride on the TiO₂ surface is greatly affected by the fluoride concentration and the solution pH because hydroxides in the solution compete with fluorides for the surface Ti⁴⁺ sites on TiO₂. Fig. 6 shows the photocatalytic activity of F-TiO₂/Pd for the degradation of urea as a function of fluoride concentration and solution pH as well as the degree of fluorination of the TiO₂ surface (i.e., the fraction of the fluorinated TiO₂ surface ($\text{Ti}-\text{F}$)), which was estimated using the surface protonation ($\text{p}K_{\text{a}1}^{\text{s}} = 3.9$ and $\text{p}K_{\text{a}2}^{\text{s}} = 8.7$) and fluorination constants ($\text{p}K_{\text{f}}^{\text{s}} = 6.2$) of TiO₂ [41]. The results are expressed in terms of the first-order degradation rate constant (k). The k value increased with increasing fluoride concentration. A higher concentration of fluorides promotes the ligand exchange reaction between fluorides in the solution and hydroxyl groups on the TiO₂ surface, thus fluorinating more of the TiO₂ surface ($\text{Ti}-\text{OH} + \text{F}^- \rightarrow \text{Ti}-\text{F} + \text{OH}^-$) (Fig. 6a). This accelerates the degradation of urea by enhancing the reaction between h_{vb}^+ and water molecules and the production of $\cdot\text{OH}$. On the other hand, the k value decreased with increasing solution pH. This trend is consistent with the fraction of the fluorinated TiO₂ surface depending on the solution pH (Fig. 6b). A higher concentration of hydroxides (i.e., more basic conditions) more significantly induces the desorption of fluorine groups from the TiO₂ surface ($\text{Ti}-\text{F} + \text{OH}^- \rightarrow \text{Ti}-\text{OH} + \text{F}^-$), diminishing the positive effect of fluoride complexation on $\cdot\text{OH}$ production and thus the urea degradation rate. Overall, the degree of TiO₂ surface fluorination is a key factor in determining the photocatalytic activity of F-TiO₂/Pd for the degradation of urea, and it increases with increasing fluoride concentration and decreasing solution pH.

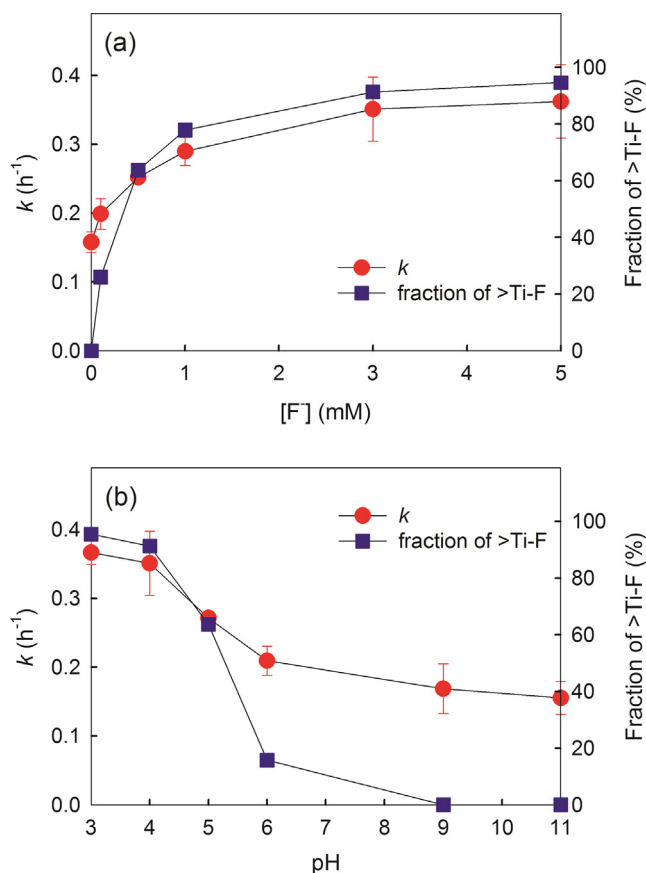


Fig. 6. Effect of (a) fluoride concentration and (b) solution pH on the degradation of urea on F-TiO₂/Pd under UV irradiation.

3.4. Practical viability of F-TiO₂/Pd for the degradation of urea

We investigated the effects of fluoride complexation on Au/TiO₂ and Pt/TiO₂ on urea degradation under UV irradiation and compared them with that on Pd/TiO₂ (Table 1). The photocatalytic degradation of urea on Au/TiO₂ and Pt/TiO₂ was better than that on bare TiO₂, which implies that, like Pd nanoparticles, Au and Pt nanoparticles also enhance the production of $\cdot\text{OH}$ by facilitating $h_{\nu\text{b}}^+$ transfer to the TiO₂ surface. The extent of the positive effect of metal loading on urea degradation increased in the order Pd < Au < Pt. However, the effect of fluoride complexation on metal-loaded TiO₂ varied considerably depending on the type of metal. Therefore, the order of the photocatalytic activities of the metal-loaded TiO₂ samples was markedly changed after fluoride complexation. The extent of the fluoride complexation effect on metal-loaded TiO₂ was expressed in terms of the relative first-order degradation rate constant ($k_{\text{rel}} = k(\text{F-TiO}_2/\text{metal})/k(\text{metal/TiO}_2)$). The

Table 1
Effect of fluoride complexation on the degradation of urea for TiO₂ loaded with different metals.

Type	k (h ⁻¹)	k_{rel}
bare TiO ₂	0.097 (± 0.008)	1.557
F-TiO ₂	0.151 (± 0.009)	
Pd/TiO ₂	0.158 (± 0.010)	2.222
F-TiO ₂ /Pd	0.351 (± 0.033)	
Au/TiO ₂	0.173 (± 0.018)	1.289
F-TiO ₂ /Au	0.223 (± 0.001)	
Pt/TiO ₂	0.240 (± 0.026)	0.688
F-TiO ₂ /Pt	0.165 (± 0.023)	

most significant positive effect of fluoride complexation was observed for the Pd/TiO₂ sample ($k_{\text{rel}} = 2.222$). Fluoride complexation on the surface of Au/TiO₂ slightly increased the degradation rate of urea ($k_{\text{rel}} = 1.289$). However, the photocatalytic activity of Pt/TiO₂ for the degradation of urea decreased upon fluoride complexation ($k_{\text{rel}} = 0.688$). The negative effect of fluoride complexation on Pt/TiO₂ should be due to the high adsorption capacity of Pt toward fluoride. It has been reported that the adsorption of halogen ions such as fluoride and chloride is especially significant on the surface of Pt nanoparticles [48,49]. Fluorides adsorbed on Pt nanoparticles hinder the adsorption of oxygen [50], which in turn inhibits electron transfer from Pt nanoparticles to oxygen and promotes surface-mediated recombination between the trapped electrons in Pt and the surface-trapped holes on TiO₂. This behavior eventually retards the degradation of urea by reducing the generation of $\cdot\text{OH}$. The concentration of fluorides adsorbed on the surface of photocatalyst was obtained by subtracting the equilibrium concentration of fluorides in the presence of photocatalyst from the initial concentration of fluorides in the absence of photocatalyst. The adsorptions of fluorides on the surfaces of bare TiO₂, Pd/TiO₂, and Pt/TiO₂ (17.5 mg/35 mL) were 140 (± 3) μM, 142 (± 5) μM, and 337 (± 18) μM, respectively, at [NaF] = 3 mM and pH = 4.0. This result indicates that the adsorption capacity of Pt toward fluoride (adsorbed [F⁻] ≈ 200 μM) is much higher than that of Pd (adsorbed [F⁻] ≈ 0 μM). It should be noted that F-TiO₂/Pd showed the highest activity for the degradation of urea among the eight photocatalysts assessed in this study (i.e., bare TiO₂ ($k = 0.097$ h⁻¹), Pd/TiO₂ ($k = 0.158$ h⁻¹), F-TiO₂ ($k = 0.151$ h⁻¹), F-TiO₂/Pd ($k = 0.351$ h⁻¹), Au/TiO₂ ($k = 0.173$ h⁻¹), F-TiO₂/Au ($k = 0.223$ h⁻¹), Pt/TiO₂ ($k = 0.240$ h⁻¹), and F-TiO₂/Pt ($k = 0.165$ h⁻¹)). Therefore, F-TiO₂/Pd can be proposed as an efficient photocatalyst for the degradation of urea.

The photocatalytic degradation of urea on F-TiO₂/Pd in urea solution was compared with that in artificial urine solution containing various chemicals (see experimental section for its chemical composition). The degradation of urea in artificial urine solution proceeded slightly more slowly than that in urea solution (Fig. 7). This result should be due to the presence of other organic compounds in artificial urine solution, which compete with urea for $\cdot\text{OH}$. However, the effects of other chemicals in artificial urine solution on the degradation of urea were minor. After 3 h of UV irradiation, 67% and 64% of urea were degraded over F-TiO₂/Pd in urea solution and artificial urine solution, respectively. This result confirms that F-TiO₂/Pd is a viable photocatalyst for the degradation of urea in human urine for water recycling on the ISS.

The stability of F-TiO₂/Pd during the photocatalytic degradation of urea was assessed over repeated cycles (Fig. 8). Urea solution or

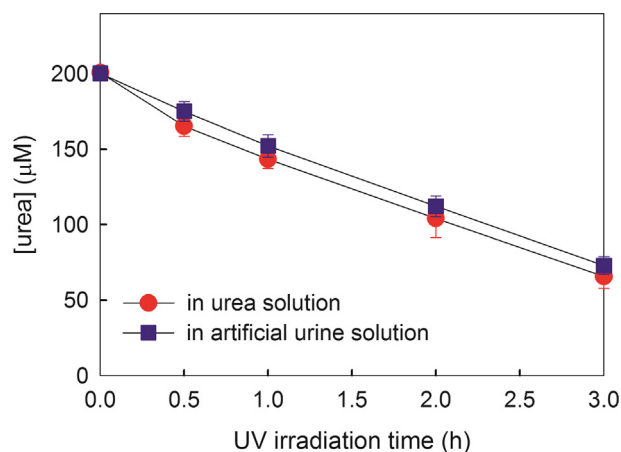


Fig. 7. Photocatalytic degradation of urea on F-TiO₂/Pd in urea solution and artificial urine solution under UV irradiation.

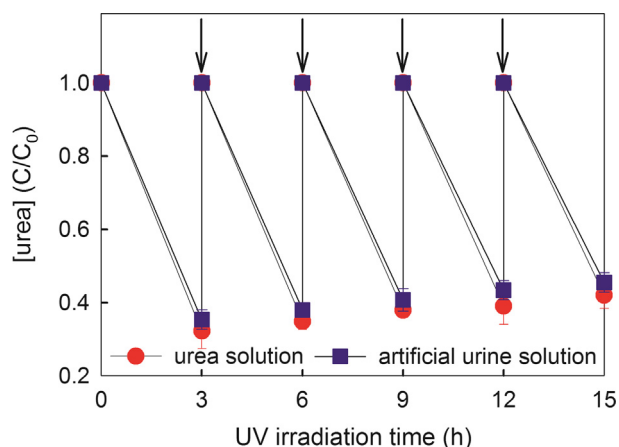


Fig. 8. Repeated cycles of urea degradation on F-TiO₂/Pd under UV irradiation. Urea solution or artificial urine solution ([urea] = 200 μM) was repeatedly added at the beginning of each cycle (i.e., every 3 h) as indicated by arrows.

artificial urine solution ([urea] = 200 μM) was added into the reactor, and the F-TiO₂/Pd suspension was stirred for 30 min prior to UV irradiation at the beginning of each cycle. The degradation efficiency of urea on F-TiO₂/Pd was largely maintained up to five cycles, which verifies the practical viability of F-TiO₂/Pd for the degradation of urea. A slight decrease in degradation efficiency with an increasing number of cycles is likely due to the physical loss of F-TiO₂/Pd powder from sampling, not to the deactivation of the F-TiO₂/Pd photocatalyst. However, it should be noted that the desorption of fluorides from the F-TiO₂/Pd surface occurs if the pH of wastewater containing urea (or urine) is high. In addition, background anions in wastewater containing urea (or urine) may replace fluorides on the surface of F-TiO₂/Pd. These behaviors reduce the photocatalytic activity of F-TiO₂/Pd for the degradation of urea. Therefore, a highly stable surface fluoride complexation method (not a simple ligand exchange method) needs to be developed.

4. Conclusions

Developing an efficient method for the degradation of urea is an important issue as there is a growing need to develop a water recycling system for the ISS, which recycles human urine into clean water. Photocatalysis is a promising and efficient method for the degradation of urea in the ISS because of the high intensity of solar radiation (especially UV radiation) available. In this work, we developed the highly efficient F-TiO₂/Pd photocatalyst for both the degradation and mineralization of urea. Surface Pd and fluoride on F-TiO₂/Pd act synergistically to enhance the production of [•]OH, which is the primary oxidant in photocatalytic urea degradation. Among the eight photocatalysts assessed in this study (i.e., bare TiO₂, Pd/TiO₂, F-TiO₂, F-TiO₂/Pd, Au/TiO₂, F-TiO₂/Au, Pt/TiO₂, and F-TiO₂/Pt), F-TiO₂/Pd exhibited the highest activity for the degradation of urea. In addition, the photocatalytic activity of F-TiO₂/Pd was largely maintained in repeated urea degradation cycles. Based on its high degradation/mineralization efficiency and stability, F-TiO₂/Pd is proposed as a viable photocatalyst for the degradation of urea, especially on the ISS.

Acknowledgments

This research was supported by Young Research Program (NRF-2016R1A1A1A05005200) and Space Core Technology Development Program (NRF-2014M1A3A3A02034875) through the National Research Foundation of Korea (NRF) funded by the Ministry of Science and ICT. This work was also supported by the Korea Polar Research Institute (KOPRI) Project (PE18200), the Korea Ministry of

Environment as Waste to Energy-Recycling Human Resource Development Project (YL-WE-17-001) and the Yonsei University Future-leading Research Initiative of 2017 (2017-22-0043).

References

- [1] K. Wenderich, G. Mul, Methods, mechanism, and applications of photodeposition in photocatalysis: a review, *Chem. Rev.* 116 (2016) 14587–14619.
- [2] W. Szeto, J. Li, H. Huang, D.Y.C. Leung, VUV/TiO₂ photocatalytic oxidation process of methyl orange and simultaneous utilization of the lamp-generated ozone, *Chem. Eng. Sci.* 177 (2018) 380–390.
- [3] L.B.B. Ndong, X. Gu, S. Lu, M.P. Ibondou, Z. Qiu, Q. Sui, S.M. Mbadanga, B. Mu, Role of reactive oxygen species in the dechlorination of trichloroethene and 1,1,1-trichloroethane in aqueous phase in UV/TiO₂ systems, *Chem. Eng. Sci.* 123 (2015) 367–375.
- [4] K. Nakata, A. Fujishima, TiO₂ photocatalysis: design and applications, *J. Photochem. Photobiol. C: Photochem. Rev.* 13 (2012) 169–189.
- [5] A. Fujishima, X. Zhang, D.A. Tryk, TiO₂ photocatalysis and related surface phenomena, *Surf. Sci. Rep.* 63 (2008) 515–582.
- [6] J. Schneider, M. Matsuoka, M. Takeuchi, J. Zhang, Y. Horiuchi, M. Anpo, D.W. Bahemmann, Understanding TiO₂ photocatalysis: mechanisms and materials, *Chem. Rev.* 114 (2014) 9919–9986.
- [7] H. Park, Y. Park, W. Kim, W. Choi, Surface modification of TiO₂ photocatalyst for environmental applications, *J. Photochem. Photobiol. C: Photochem. Rev.* 15 (2013) 1–20.
- [8] J. Zhang, G. Xiao, F.-X. Xiao, B. Liu, Revisiting one-dimensional TiO₂ based hybrid heterostructures for heterogeneous photocatalysis: a critical review, *Mater. Chem. Front.* 1 (2017) 231–250.
- [9] M.G. Méndez-Medrano, E. Kowalska, A. Lehoux, A. Herisson, B. Ohtani, D. Bahena, V. Briois, C. Colbeau-Justin, J.L. Rodríguez-López, H. Remita, Surface modification of TiO₂ with Ag nanoparticles and CuO nanoclusters for application in photocatalysis, *J. Phys. Chem. C* 120 (2016) 5143–5154.
- [10] W. Choi, Pure and modified TiO₂ photocatalysts and their environmental applications, *Catal. Surv. Asia* 10 (2006) 16–28.
- [11] A. Ayati, B. Tanhaei, F.F. Bamoharran, A. Ahmadpour, P. Maydannik, M. Sillanpää, Photocatalytic degradation of nitrobenzene by gold nanoparticles decorated polyoxometalate immobilized TiO₂ nanotubes, *Sep. Purif. Technol.* 171 (2016) 62–68.
- [12] L. Ling, C. Wang, M. Ni, C. Shang, Enhanced photocatalytic activity of TiO₂/single-walled carbon nanotube (SWCNT) composites under UV-A irradiation, *Sep. Purif. Technol.* 169 (2016) 273–278.
- [13] W. Chen, X. Ran, X. Jiang, H. Min, D. Li, L. Zou, J. Fan, G. Li, Synthesis of TiO₂ and TiO₂-Pt and their application in photocatalytic degradation of humic acid, *Water Environ. Res.* 86 (2014) 48–55.
- [14] A. Ofiarska, A. Pieczyńska, A.F. Borzyszkowska, P. Stepnowski, E.M. Siedlecka, Pt-TiO₂-assisted photocatalytic degradation of the cytostatic drugs ifosfamide and cyclophosphamide under artificial sunlight, *Chem. Eng. J.* 285 (2016) 417–427.
- [15] I. Dobrosz-Gómez, M.Á. Gómez-García, S.M. López-Zamora, E. GilPavas, J. Bojarska, M. Kozanecki, J.M. Rynkowski, Transition metal loaded TiO₂ for phenol photo-degradation, *C. R. Chim.* 18 (2015) 1170–1182.
- [16] D. Zhao, C. Chen, Y. Wang, H. Ji, W. Ma, L. Zang, J. Zhao, Surface modification of TiO₂ by phosphate: effect on photocatalytic activity and mechanism implication, *J. Phys. Chem. C* 112 (2008) 5993–6001.
- [17] Y. Wang, L. Li, X. Huang, Q. Li, G. Li, New insights into fluorinated TiO₂ (brookite, anatase and rutile) nanoparticles as efficient photocatalytic redox catalysts, *RSC Adv.* 5 (2015) 34302–34313.
- [18] G.W. Park, M. Cho, E.L. Cates, D. Lee, B.-T. Oh, J. Vinjé, J.-H. Kim, Fluorinated TiO₂ as an ambient light-activated virucidal surface coating material for the control of human norovirus, *J. Photochem. Photobiol. B: Biol.* 140 (2014) 315–320.
- [19] A. Vijayabalan, K. Selvam, R. Velmurugan, M. Swaminathan, Photocatalytic activity of surface fluorinated TiO₂-P25 in the degradation of reactive orange 4, *J. Hazard. Mater.* 172 (2009) 914–921.
- [20] A. Yamakata, T.-a. Ishibashi, H. Onishi, Water- and oxygen-induced decay kinetics of photogenerated electrons in TiO₂ and Pt/TiO₂: a time-resolved infrared absorption study, *J. Phys. Chem. B* 105 (2001) 7258–7262.
- [21] H. Park, W. Choi, Effects of TiO₂ surface fluorination on photocatalytic reactions and photoelectrochemical behaviors, *J. Phys. Chem. B* 108 (2004) 4086–4093.
- [22] J. Kim, W. Choi, Hydrogen producing water treatment through solar photocatalysis, *Energy Environ. Sci.* 3 (2010) 1042–1045.
- [23] J. Kim, D. Monllor-Satoca, W. Choi, Simultaneous production of hydrogen with the degradation of organic pollutants using TiO₂ photocatalyst modified with dual surface components, *Energy Environ. Sci.* 5 (2012) 7647–7656.
- [24] S. Weon, J. Kim, W. Choi, Dual-components modified TiO₂ with Pt and fluoride as deactivation-resistant photocatalyst for the degradation of volatile organic compound, *Appl. Catal. B: Environ.* 220 (2018) 1–8.
- [25] P.M. Glibert, J. Harrison, C. Heil, S. Seitzinger, Escalating worldwide use of urea - a global change contributing to coastal eutrophication, *Biogeochemistry* 77 (2006) 441–463.
- [26] E.R. Blatchley, M. Cheng, Reaction mechanism for chlorination of urea, *Environ. Sci. Technol.* 44 (2010) 8529–8534.
- [27] A.N. Rollinson, J. Jones, V. Dupont, M.V. Twigg, Urea as a hydrogen carrier: a perspective on its potential for safe, sustainable and long-term energy supply, *Energy Environ. Sci.* 4 (2011) 1216–1224.
- [28] C. Rose, A. Parker, B. Jefferson, E. Cartmell, The characterization of feces and urine: a review of the literature to inform advanced treatment technology, *Crit. Rev.*

- Environ. Sci. Technol. 45 (2015) 1827–1879.
- [29] L.S. Bobe, A.A. Kochetkov, V.A. Soloukhin, M.J. Tomashpolskiy, P.O. Andreichuk, N.N. Protasov, J.E. Sinyak, Water recovery and urine collection in the russian orbital segment of the international space station (mission 1 through mission 17), *SAE Int. J. Aerosp.* 4 (2011) 401–409.
- [30] B.B. Tolar, N.J. Wallsgrove, B.N. Popp, J.T. Hollibaugh, Oxidation of urea-derived nitrogen by thaumarchaeota-dominated marine nitrifying communities, *Environ. Microbiol.* 19 (2017) 4838–4850.
- [31] H. Li, Q. Yu, B. Yang, Z. Li, L. Lei, Electro-catalytic oxidation of artificial human urine by using BDD and IrO₂ electrodes, *J. Electroanal. Chem.* 738 (2015) 14–19.
- [32] H. Zöllig, A. Remmele, C. Fritzsche, E. Morgenroth, K.M. Udert, Formation of chlorination byproducts and their emission pathways in chlorine mediated electro-oxidation of urine on active and nonactive type anodes, *Environ. Sci. Technol.* 49 (2015) 11062–11069.
- [33] E. Nicolau, I. González-González, M. Flynn, K. Griebenow, C.R. Cabrera, Bioelectrochemical degradation of urea at platinumized boron doped diamond electrodes for bioregenerative systems, *Adv. Space Res.* 44 (2009) 965–970.
- [34] E. Nicolau, J.J. Fonseca, J.A. Rodríguez-Martínez, T.-M.J. Richardson, M. Flynn, K. Griebenow, C.R. Cabrera, Evaluation of a urea bioelectrochemical system for wastewater treatment processes, *ACS Sustain. Chem. Eng.* 2 (2014) 749–754.
- [35] S. Kim, G. Piao, D.S. Han, H.K. Shon, H. Park, Solar desalination coupled with water remediation and molecular hydrogen production: a novel solar water-energy nexus, *Energy Environ. Sci.* 11 (2018) 344–353.
- [36] S. Park, J.T. Lee, J. Kim, Photocatalytic oxidation of urea on TiO₂ in water and urine: mechanism, product distribution, and effect of surface platinumization, *Environ. Sci. Pollut. Res.* (2017), <https://doi.org/10.1007/s11356-11017-18380-11353>.
- [37] E. Pelizzetti, P. Calza, G. Mariella, V. Maurino, C. Minero, H. Hidaka, Different photocatalytic fate of amido nitrogen in formamide and urea, *Chem. Commun.* (2004) 1504–1505.
- [38] X. Jiang, M. Manawan, T. Feng, R. Qian, T. Zhao, G. Zhou, F. Kong, Q. Wang, S. Dai, J.H. Pan, Anatase and rutile in evonik aerioxide P25: heterojunctioned or individual nanoparticles? *Catal. Today* 300 (2018) 12–17.
- [39] J.A. Wilsenach, C.A.H. Schuurbiers, M.C.M. van Loosdrecht, Phosphate and potassium recovery from source separated urine through struvite precipitation, *Water Res.* 41 (2007) 458–466.
- [40] J. Lee, W. Choi, Effect of platinum deposits on TiO₂ on the anoxic photocatalytic degradation pathways of alkylamines in water: dealkylation and N-alkylation, *Environ. Sci. Technol.* 38 (2004) 4026–4033.
- [41] C. Minero, G. Mariella, V. Maurino, E. Pelizzetti, Photocatalytic transformation of organic compounds in the presence of inorganic anions. I. Hydroxyl-mediated and direct electron-transfer reactions of phenol on a titanium dioxide-fluoride system, *Langmuir* 16 (2000) 2632–2641.
- [42] C.G. Hatchard, C.A. Parker, A new sensitive chemical actinometer. II. Potassium ferrioxalate as a standard chemical actinometer, *Proc. R. Soc. London Ser. A: Math. Phys. Eng. Sci.* 235 (1956) 518–536.
- [43] M. Revilla, J. Alexander, P.M. Glibert, Urea analysis in coastal waters: comparison of enzymatic and direct methods, *Limnol. Oceanogr. Meth.* 3 (2005) 290–299.
- [44] K.-i. Ishibashi, A. Fujishima, T. Watanabe, K. Hashimoto, Detection of active oxidative species in TiO₂ photocatalysis using the fluorescence technique, *Electrochem. Commun.* 2 (2000) 207–210.
- [45] N. Li, M. Liu, B. Yang, W. Shu, Q. Shen, M. Liu, J. Zhou, Enhanced photocatalytic performance toward CO₂ hydrogenation over nanosized TiO₂-loaded Pd under UV irradiation, *J. Phys. Chem. C* 121 (2017) 2923–2932.
- [46] J. Tang, H. Quan, J. Ye, Photocatalytic properties and photoinduced hydrophilicity of surface-fluorinated TiO₂, *Chem. Mater.* 19 (2007) 116–122.
- [47] J. Ryu, W. Kim, J. Kim, J. Ju, J. Kim, Is surface fluorination of TiO₂ effective for water purification? The degradation vs. mineralization of phenolic pollutants, *Catal. Today* 282 (2017) 24–30.
- [48] L. Nie, P. Zhou, J. Yu, M. Jaroniec, Deactivation and regeneration of Pt/TiO₂ nanosheet-type catalysts with exposed (0 0 1) facets for room temperature oxidation of formaldehyde, *J. Mol. Catal. A: Chem.* 390 (2014) 7–13.
- [49] F.J. Gracia, J.T. Miller, A.J. Kropf, E.E. Wolf, Kinetics, FTIR, and controlled atmosphere EXAFS study of the effect of chlorine on Pt-supported catalysts during oxidation reactions, *J. Catal.* 209 (2002) 341–354.
- [50] X. Zhu, B. Cheng, J. Yu, W. Ho, Halogen poisoning effect of Pt-TiO₂ for formaldehyde catalytic oxidation performance at room temperature, *Appl. Surf. Sci.* 364 (2016) 808–814.